ELSEVIER

Chemical Engineering Journal 80 (2000) 119–133

Chemical Engineering Journal

www.elsevier.com/locate/cej

On boundary conditions and solutions for ideal clarifier–thickener units

Stefan Diehl*

Centre for Mathematical Sciences, Lund University, P.O. Box 118, SE-221 00 Lund, Sweden

Abstract

Solid–liquid separation by the process of continuous sedimentation in a clarifier–thickener unit, or settler, is difficult to model. Simplified assumptions on the behaviour of the solids, the flows, the physical design of the settler, etc. still leave the fundamental process highly non-linear. A fairly simple model consists of a one-dimensional settler, with a constant or varying cross-sectional area, in which an ideal suspension of solids behaves according to the Kynch assumption (the settling velocity is a function of the local concentration only) and the conservation of mass. At the bottom of the settler the concentration increases with depth as a result of, among other things, compression and a converging cross-sectional area. It is important to understand fully the mathematical implications of the simplified assumptions before investigating more complex models. In this paper it is demonstrated what impact a converging cross-sectional area has on the increase in concentration at the bottom for incompressible suspensions (a consequence of Kynch's assumption). This analysis leads to a natural boundary condition at the bottom, which is a special case of a generalized entropy condition for the type of partial differential equation under consideration. The mathematical problems concerning the boundary conditions at the top, bottom and inlet are resolved uniquely by this generalized entropy condition. One aim of the paper is to describe and elucidate this condition by examples leaving out some technical mathematical details. The construction of a unique solution, including the prediction of the outlet concentrations, is described by examples in the case of a constant cross-sectional area. Comparisons with numerical solutions are also presented.

Keywords: Continuous sedimentation; Clarifier; Thickener; Settler; Boundary conditions; Settling

1. Introduction

Continuous sedimentation, where gravity is the driving force, is a commonly used solid–liquid separation process in various industrial applications. It takes place in a clarifier–thickener unit or settler, which has one inlet (somewhere in the middle) and two outlets (at the top and bottom). For mathematical modelling purposes we consider ideal settlers shown in Fig. 1. The concept of the ideal thickener was introduced and analysed by Shannon and Tory [31]. The settlers are ideal in the sense that the concentration distribution is influenced only by the conservation of mass in one dimension, perhaps with a varying cross-sectional area, together with a constitutive assumption on the gravity settling. This means that the concentration is assumed to be constant on each cross-section, the inlet is modelled by a point source and the solids leaving the inlet are distributed instantaneously and evenly over the entire cross-section. Analogously, the solids leaving the settler at the outlets are taken instantaneously from the entire cross-section. Such phenomena as turbulence and wall effects are neglected. We also assume that sedimentation takes place only inside the settler. Thus, in the inlet and outlet pipes the relative velocity between the solids and the liquid is assumed to be zero.

The basic constitutive assumption for the settling of solids is the one by Kynch [25]: the flux of particles per unit area and time is a function of the concentration only. It is valid for non-flocculated dispersions of solid particles all of the same size and shape, which show no compressible behaviour at any concentration and for which diffusion phenomena are so small that they can be neglected; cf. experiments reported in [11,15]. Kynch's assumption together with the conservation of mass written as a hyperbolic partial differential equation, interpreted in the weak sense (distribution sense), makes it possible to capture the main feature of sedimentation — the movement of large concentration gradients (shock waves). The construction of solutions by the method of characteristics describing sedimentation in the thickening zone or in batch mode can be found in, for example [5–7,21,25,29,30].

To model the sedimentation behaviour of a wider class of suspensions more refined assumptions need to be considered. In particular, the modelling of the compressible behaviour of flocculated suspensions at high concentrations

* Fax: +46-46-2224010.
E-mail address: diehl@maths.lth.se (S. Diehl).

1383-5866/00/$ – see front matter
PII: S1383-5866(00)00081-2

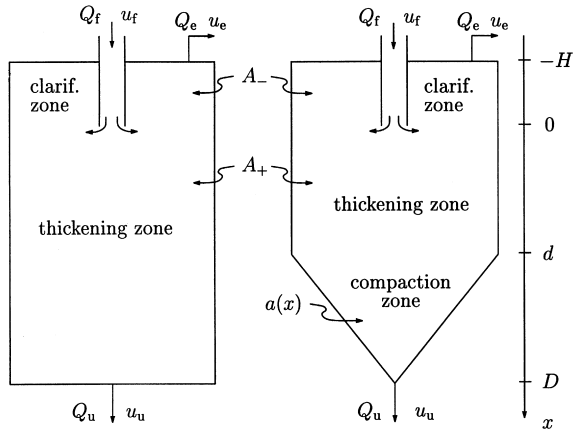

Fig. 1. Two ideal clarifier–thickener units. The indices are e=effluent, f=feed and u=underflow.

has attracted much attention. As shown in [1,3,4,14] sedimentation with compression can be modelled with a single partial differential equation including a non-linear diffusion term, and can thus be seen as a direct extension of the Kynch assumption.

At the bottom of the settler the concentration increases with depth as a result of, among other things, compression and a converging cross-sectional area. In this paper it is demonstrated what impact a converging cross-sectional area has on the increase in concentration at the bottom for incompressible suspensions (a consequence of Kynch's assumption). The results agree with those obtained by Shannon and Tory [31], who calculated the exact steady-state profiles for a settler with a conical bottom region as in Fig. 1(right). For a flat bottom there is a jump between the concentration at the bottom inside the settler and the concentration in the outlet pipe. We emphasize that this refers to a one-dimensional ideal model and is a consequence of the conservation of mass and the assumption that there is sedimentation inside the settler but not in the outlet pipe. Early work by Comings et al. [12,13] and recent work by Farrow et al. [23] show that jumps do occur at the outlet. In reality mechanical rake action and flows in more than one dimension influence the concentrations, especially in the case of a flat bottom or one with a low slope. With a cross-sectional area that decreases with depth there is some possibility of maintaining a constant concentration at a given height. If the slope is great enough, solids approaching the slanted side will slide along the incline, displacing fluid in the interior. For a flat or low-sloped bottom rakes are normally used to draw solids to the outlet. If no rakes are used, a natural cone (at the angle of repose) of solids builds up around the outlet. Only the solids in this inner cone move through the system. Hence, the settler works as if it had a decreasing cross-sectional area with greater slopes.

The aim of the modelling of the entire clarifier–thickener unit is to predict the two outlet concentrations and the concentration distribution within the vessel given any loading conditions, that is, given the feed concentration of the inlet, the three volume flows and an initial concentration distribution only within the settler. In particular, it is important to predict the behaviour of the large discontinuity (the sludge blanket in waste water treatment) that appears under normal operating conditions. We also emphasize that the boundary concentrations at the top and bottom of the settler and just above and below the feed inlet are parts of the solution and cannot be prescribed.

Under the ideal physical assumptions described above and the Kynch assumption, the entire clarifier–thickener unit can be described completely by a single partial differential equation with point source and discontinuous flux function; see [17,19]. This type of equation has the advantage that it is possible to construct solutions by the method of characteristics, at least for piecewise constant initial data and a constant cross-sectional area. The disadvantage is that non-uniqueness of solution occurs due to the formation of discontinuities. In order to resolve this mathematical problem of non-uniqueness so called entropy conditions must be introduced. They relate fluxes and concentrations at discontinuities.

For example, within the clarification or the thickening zone, the entropy condition by Oleinik [27,28] should be used. It can be written as an inequality involving the same flux function on both sides of the discontinuity. It can be motivated (physically and mathematically) by introducing a small amount of diffusion, which is not included in the idealized assumption by Kynch. This is called a viscous profile analysis, see e.g. Smoller [32]. The outcome is that unstable discontinuities are rejected and for each allowed discontinuity the jump condition determines uniquely the speed of the discontinuity, which is a function of the concentration values on each side of it.

The conservation of mass at the top, bottom and inlet of the settler yields jump conditions that involve different flux functions on either side of these three discontinuities, which all have the speed zero by the physical configuration. The six boundary concentrations on either side of these discontinuities are not uniquely determined by the three jump equations. To pick out a unique solution a generalized entropy condition, condition Γ, is introduced by the author in [16]. These boundary values cannot be given beforehand, but are a natural part of the solution. Because of the different (non-linear) flux functions on either side of these discontinuities, the situation is much more complicated than at a discontinuity within the clarification or thickening zone. The boundary concentrations may be discontinuous functions of time, creating discontinuities that move into the clarification or thickening zone.

The investigation of the dynamic and steady-state behaviour of the entire settler (with constant or varying cross-sectional area) by means of solutions of partial differential equations has been done by Chancelier et al. [10] and the author in [17,19]. In the case of a constant cross-sectional area a procedure of construction of solutions by means of

the method of characteristics together with condition Γ is presented in [17]. However, that paper contains technical mathematical details that are not of interest for those who are primarily interested in sedimentation and, furthermore, the procedure of construction of solution was primarily introduced in order to show existence of a solution.

One purpose of this article is to describe condition Γ with fewer technical details than in [17]. This will be done in connection with the description of the concentration distribution at the bottom of a settler with converging cross-sectional area. Then it is exemplified how analytical solutions can be constructed.

2. Ideal clarifier–thickener units and the conservation law

Let $u(x, t)$ denote the (unknown) concentration of solid particles (mass per unit volume), where t is the time and x is the depth from the feed inlet. Let $A(x)$ denote the cross-sectional area. In this paper we shall investigate two ideal settler models shown in Fig. 1. The right settler model has the cross-sectional area:

$$A(x) = \begin{cases} A_-, & -H \le x < 0 \\ A_+, & 0 < x < d \\ a(x), & d \le x \le D, \end{cases}$$

where $a(x)$ satisfies $a(d) = A_+$ and $a'(x) < 0$. We designate the region (interval) (d, D) the compaction zone (not compression zone) because of, as we shall demonstrate, the concentration increase due to the decreasing cross-sectional area. The left settler model is the limit of the right one as $d \to D$. The height of the clarification zone is H for both models, the depths of the thickening zones are D and d for the left and right model, respectively. The directions of the known volume flows Q_f, Q_e and Q_u (volume per unit time) are shown in the figure. The known concentration of the feed inlet is denoted by $u_\mathrm{f}(t)$ and the unknown concentrations of the outlets at the top and bottom are denoted by $u_\mathrm{e}(t)$ and $u_\mathrm{u}(t)$, respectively.

According to the constitutive assumption by Kynch [25] the settling velocity of the solids due to gravity in a batch settling column is a function of the local concentration only; $v_\mathrm{settl}(u)$. Note that $u = \phi\rho_\mathrm{s}$, where ϕ denotes the volume fraction of solids and ρ_s their density. The batch settling flux (mass per unit time and unit area) is denoted by $f_\mathrm{b}(u) = v_\mathrm{settl}(u)u$ and is assumed to have the form shown in Fig. 2. The maximum packing concentration is denoted by $u_\mathrm{max}$and the only inflection point by u_infl.

Consider the interior of the thickening zone with the constant cross-sectional area A_+. The bulk velocity is defined as:

$$v = \frac{Q_\mathrm{u}}{A_+}.$$

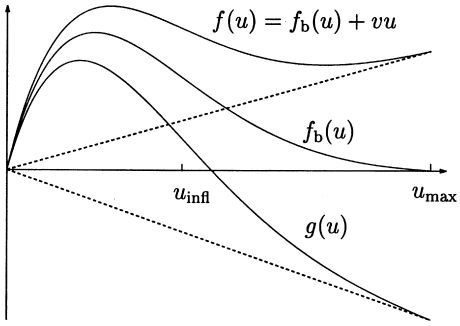

Fig. 2. The flux curves f_b, f and g. The dashed lines have the slopes $v{=}Q_\mathrm{u}/A_+$, and $-Q_\mathrm{e}/A_+$, respectively. Note that the inflection point u_infl is the same for the three flux functions.

The conservation of mass can be written as the partial differential equation (conservation law):

$$\frac{\partial u}{\partial t} + \frac{\partial (v_\mathrm{s} u)}{\partial x} = 0, \tag{1}$$

where v_s is the velocity of the solids. If v_l denotes the liquid velocity, then the bulk velocity can be written:

$$v = v_\mathrm{s}\phi + v_\mathrm{l}(1-\phi) = v_\mathrm{s} - (v_\mathrm{s} - v_\mathrm{l})(1-\phi). \tag{2}$$

Here, the last term is actually the batch settling velocity. In batch sedimentation $v = 0$ hence Eq. (2) yields $v_\mathrm{s} = (v_\mathrm{s} - v_\mathrm{l})(1-\phi) \equiv v_\mathrm{settl}$ which by Kynch's assumption is a function only of $u(= \rho_\mathrm{s}\phi)$. Thus, Eq. (2) can be written $v_\mathrm{s}(u) = v_\mathrm{settl}(u) + v$ and the flux function of Eq. (1) can be expressed as:

$$f(u) = v_\mathrm{s}(u)u = (v_\mathrm{settl}(u) + v)u = f_\mathrm{b}(u) + vu.$$

Eq. (1) can be written:

$$\frac{\partial u}{\partial t} + f'(u)\frac{\partial u}{\partial x} = 0, \tag{3}$$

which is a quasi-linear partial differential equation with the property that a constant concentration u_0 propagates with the speed $f'(u_0)$ in an x–t coordinate plane; cf. Kynch [25]. These straight lines of constant concentration are called characteristics. Two characteristics with different concentration values carrying initial data from the x-axis (at $t = 0$) may intersect and then a discontinuity appears. The jump condition for a discontinuity $x = x(t)$ having the concentration values u^{x-} and u^{x+} on the left and right side, respectively, is:

$$x'(t) = \frac{f(u^{x+}) - f(u^{x-})}{u^{x+} - u^{x-}}$$

and the entropy condition by Oleinik [27,28] is:

$$\frac{f(\alpha) - f(u^{x-})}{\alpha - u^{x-}} \ge \frac{f(u^{x+}) - f(u^{x-})}{u^{x+} - u^{x-}} \quad \text{for all } \alpha \text{ between } u^{x-} \text{ and } u^{x+}. \tag{4}$$

This condition means that the graph of $f(u)$ lies above (below) the chord joining the points $(u^{x-}, f(u^{x-}))$ and

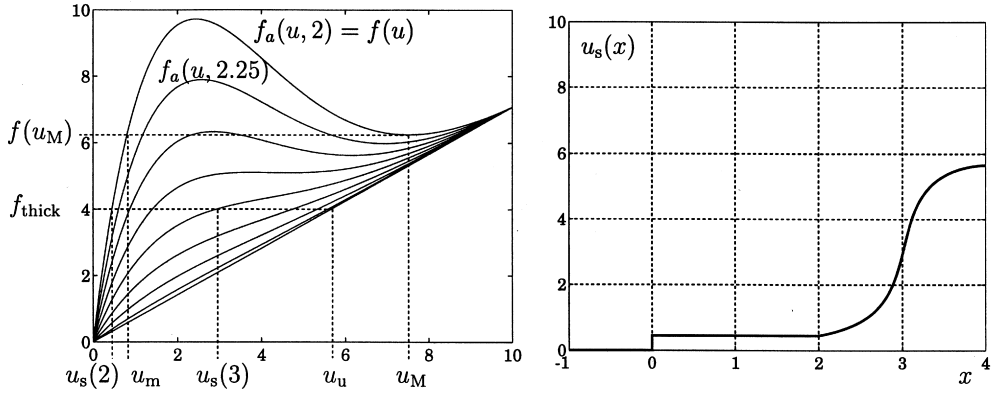

Fig. 3. Left: flux functions at $x=d=2$ m (the uppermost curve), $x=D=4$ m (the bottom-most curve) and at seven intermediate equidistant x-values. Right: the steady-state solution when $f_{thick}=4$ kg/(m^2 h) and the flux in the clarification zone is zero. The underflow concentration is $u_u=f_{thick}/v=5.65$ kg/m^3, which is only negligibly higher than the bottom concentration, since $a(D)/Q_u\approx 0$.

$(u^{x+},\ f(u^{x+}))$ when u^{x-} is less (greater) than u^{x+}. As for the examples of this paper it is assumed that the reader is familiar with the concepts above and the method of characteristics, see e.g. [26,32].

Assuming that the particles follow the liquid outside the settler, the mass per unit time entering it is $Q_f u_f(t)$ and leaving it is at the effluent $Q_e u_e(t)$ and through the underflow pipe $Q_u u_u(t)$. Extend the function $A(x)$ continuously to the whole x-axis by letting $A(x)=A(-H)$ for $x<-H$ and $A(x)=A(D)$ for $x>D$. Then the conservation of mass for the entire settler can be written:

$$\frac{\partial}{\partial t}\,(A(x)u)+\frac{\partial}{\partial x}\,(F_0(u,\,x))=Q_f u_f(t)\delta(x), \tag{5}$$

where $\delta(x)$ is the delta function and the flux function (mass flux per unit time) is:

$$F_0(u,\,x)=\begin{cases} -Q_e u, & x<-H\\ A(x)f_b(u)-Q_e u, & -H<x<0\\ A(x)f_b(u)+Q_u u, & 0<x<D\\ Q_u u, & x>D. \end{cases}$$

Here, natural flux functions appear above and below the settler. Analyses of the dynamic and steady-state behaviour of Eq. (5) have been presented by Chancelier et al. [8–10] and by the author in [19]. Normalizing Eq. (5) by dividing by $A_+=A(0+)$ gives:

$$\frac{A(x)}{A_+}\,\frac{\partial u}{\partial t}+\frac{\partial}{\partial x}(F(u,\,x))=s(t)\delta(x),$$

with the source function (mass per unit time and unit area):

$$s(t)=Q_f u_f(t)\cdot A_+$$

and the flux function $F(u,x)=F_0(u,x)/A_+$. For the right settler model this is:

$$F(u,\,x)=\begin{cases} -\dfrac{Q_e}{A_+}\,u\equiv g_e(u), & x<-H\\ \dfrac{A_-}{A_+}\,f_b(u)-\dfrac{Q_e}{A_+}\,u\equiv g(u), & -H<x<0\\ f_b(u)+vu=f(u), & 0\le x\le d\\ \dfrac{a(x)}{A_+}\,f_b(u)+vu\equiv f_a(u,\,x), & d\le x\le D\\ vu\equiv f_u(u), & x>D, \end{cases} \tag{6}$$

where we have defined the flux function g in the clarification zone (see Fig. 2), f_a in the compaction zone (see Fig. 3) and the outlet fluxes g_e and f_u. These flux functions differ from those in [19], which were obtained by normalizing by $A(x)$ instead. This can only be done for functions $A(x)$ that are continuous at $x=-H,\ 0,\ D$ because of the discontinuities of the flux function $F_0(u,\,\cdot)$ and the delta function in Eq. (5). In the present paper we allow $A(x)$ to be discontinuous at $x=0$). All fluxes are positive in the direction of the x-axis. Note also that the bulk velocity in the clarification zone is $-Q_e/A_-$ not $-Q_e/A_+$.

Since we are dealing with discontinuous weak solutions [1] $u(x,\,t)$ of partial differential equations the boundary concentrations:

$$u_-(t)=\lim_{\varepsilon\searrow 0}u(-\varepsilon,\,t),\qquad u_+(t)=\lim_{\varepsilon\searrow 0}u(\varepsilon,\,t),$$

$$u_H(t)=\lim_{\varepsilon\searrow 0}u(-H+\varepsilon,\,t),\qquad u_D(t)=\lim_{\varepsilon\searrow 0}u(D-\varepsilon,\,t),$$

will also be discontinuous. In order to state formulae that should hold pointwise (at every fixed time t) we have to define the following additional limits at each boundary:

$$u^-(t)=\lim_{\varepsilon\searrow 0}u_-(t+\varepsilon),\qquad u^+(t)=\lim_{\varepsilon\searrow 0}u_+(t+\varepsilon),$$

$$u^H(t)=\lim_{\varepsilon\searrow 0}u_H(t+\varepsilon),\qquad u^D(t)=\lim_{\varepsilon\searrow 0}u_D(t+\varepsilon).$$

[1] Some technical regularity assumptions on piecewise smoothness and monotonicity are supposed to be satisfied, see [17].

These four boundary functions are continuous from the right and we define this to hold for $u_f(t)$ (hence $s(t)$), too. The unknown functions $u_e(t)$ and $u_u(t)$ will automatically be continuous from the right by the definitions that will follow. At the feed inlet, $x = 0$, the conservation law yields the jump condition:

$$Q_f u_f(t) = A_+ f_b\left(u^+(t)\right) + Q_u u^+(t) - \left(A_- f_b\left(u^-(t)\right) - Q_e u^-(t)\right) \Leftrightarrow f\left(u^+(t)\right) = g\left(u^-(t)\right) + s(t) \tag{7}$$

and at the outlets we get:

$$-Q_e u_e(t) = A_- f_b\left(u^H(t)\right) - Q_e u^H(t) \Leftrightarrow$$
$$g_e\left(u_e(t)\right) = g\left(u^H(t)\right) \tag{8}$$

and

$$Q_u u_u(t) = A(D) f_b\left(u^D(t)\right) + Q_u u^D(t) \Leftrightarrow$$
$$f_u\left(u_u(t)\right) = \begin{cases} f\left(u^D(t)\right) & \text{(left model)} \\ f_a\left(u^D(t),\ D\right) & \text{(right model)}. \end{cases} \tag{9}$$

3. Obtaining unique boundary concentrations

The three jump conditions (Eqs. (7)–(9)) relate six boundary concentrations within and outside the settler. They are all parts of the solution of the problem of determining the behaviour of an ideal clarifier–thickener unit. As in the case of a discontinuity within the thickening zone — the jump condition (Eq. (3)) is not sufficient to determine a unique solution for given initial data — the jump conditions in Eqs. (7)–(9) do not determine the boundary concentrations (hence the concentration distribution within the settler) uniquely for given initial data and feed concentration $u_f(t)$. A uniqueness condition that picks out the physically correct boundary concentrations for rather general flux functions (with many inflection points) was introduced in [16] and called condition Γ. This is a generalization of Oleinik's entropy condition (Eq. (4)). It is motivated physically by a conservative numerical method (Godunov [24]) and by analysis of viscous profiles and their stability; see [16,18,22]. In this section condition Γ will be motivated and explained by starting with a physical/mathematical discussion about the jump condition (Eq. (9)).

3.1. Concentrations and fluxes in the compaction zone at steady state

The conservation law for the compaction zone of the right model of Fig. 1, i.e. the interval $d < x < D$ is:

$$\frac{a(x)}{A_+}\frac{\partial u}{\partial t} + \frac{\partial}{\partial x}\left(f_a(u, x)\right) = 0, \quad d < x < D. \tag{10}$$

The characteristics (in the x–t plane) of this equation are not straight lines and the concentration values carried by these are not constant. In consequence, characteristics cannot easily be used to construct a solution without numerical calculations, not even to obtain a steady-state solution. Let $A_+ f_{thick}$ denote the steady-state flux (mass per time unit) in the thickening zone (this is denoted by Φ_{thick} in [19]). Hence, f_{thick} is the flux per unit area. The steady-state solution $u = u_s(x)$ of Eq. (10) satisfies:

$$f_a(u, x) \equiv \frac{a(x)}{A_+} f_b(u) + vu = f_{thick}. \tag{11}$$

The following facts hold for $u_s(x)$ in the case with $a'(x) < 0$ (and $Q_u > 0$ (see [19]):

- $u_s(x)$ is uniquely determined by f_{thick}.
- If u_s is constant, then either $u_s \equiv 0$ ($f_{thick} = 0$) or $u_s \equiv u_{max}$ ($f_{thick} = f(u_{max})$).
- If u_s is not constant, then it is strictly increasing with depth with at most one discontinuity.

We also mention that there is at most one discontinuity at steady state in the whole interval $0 < x < D$. For the specific value $f_{thick} = f(u_M)$ the discontinuity can be located anywhere in $0 \le x \le d$ since the cross-sectional area is constant there. Here, u_M is the concentration value of the local minimum of f (see Fig. 3). Let u_m denote the concentration less than u_M satisfying $f(u_m) = f(u_M)$.

3.1.1. Numerical values used in the figures

In order to show graphs of numerical calculations of solutions the following numerical values are used throughout the paper:

$H = 1$ m
$d = 2$ m (except in Fig. 19)
$D = 4$ m
$A_+ = \pi 30^2$ m^2
$A_- = A_+ - \pi 2^2$ m^2
$u_{infl} = 4.15$ kg/m^3
$u_{max} = 10$ kg/m^3
$u_m = 0.80$ kg/m^3
$u_M = 7.50$ kg/m^3
$Q_u = 2000$ m^3/h
$f(u_M) = 6.25\ 1$ kg/(m^{2}h)
$Q_e = 2500$m^3/h (from Section 3.3 on)
$Q_f = 4500$m^3/h (from Section 3.3 on)

The feed concentration u_f will have different values in the examples. For the compaction zone of the right settler model we have chosen $a(x) = \pi(30 - 14.75(x-2)^2)$ m^2, $2 \le x \le 4$ hence, $A(2) = A_+$ and $A(4) = \pi 0.5^2$ m^2.

In Fig. 3 $f_a(u, x)$ is plotted as a function of u for different values of the depth x. We shall now investigate the steady-state solution for different values of f_{thick}. Note that this is the flux at every point x in the interval $d < x < D$. For low values of f_{thick} there is a unique intersection with

the flux function $f(u)$, hence the concentration in the thickening zone $u_s(d) < u_m$ (see Fig. 3). We assume that the effluent flow Q_e is sufficiently low so that the concentration, and the flux, in the clarification zone is zero. The figure shows that for every given $x_0 \in [d, D]$ there is a unique intersection between the flux curve $f_a(u, x_0)$ and the horizontal line with the flux value f_{thick}. This intersection defines uniquely the concentration $u = u_s(x_0)$ as the solution of $f_a(u, x_0) = f_{thick}$. In this way, we can clearly see that the concentration is increasing with depth, following the family of flux curves $f_a(\cdot, x)$ with x as the parameter.

If $a(D)$ is close to zero, then $f_a(u, D) \approx vu$ which means that the sedimentation becomes negligible (the relative velocity between liquid and solids is zero). Note that the jump condition (Eq. (9)) (for the right settler model) implies:

$$u_u = u_D + \frac{a(D)}{Q_u} f_b(u_D).$$

For an ideal model we may let $a(D) = 0$ which implies that $f_a(u, D) = vu$ and, hence, $u_u = u_D$.

Next we consider a case with a slightly higher flux $f_{thick} = 5.63$ kg/m^2) and still $u_s(2) < u_m$ (see Fig. 4). As in the previous case there is a unique intersection between each flux curve $f_a(\cdot, x)$ for every fixed $x \in [2, 2.5)$ and the horizontal line with the flux value f_{thick}. At $x = 2.5$ m there are two intersections. The unique solution makes a jump from the concentration $u_s(2.5-0) = 1.62$ to $u_s(2.5+0) = 6.15$ and then, for $x \in (2.5, 4]$ increases continuously again. The discontinuity satisfies both the jump condition (Eq. (3)) and the entropy condition (Eq. (4)) (the graph of $f_a(u, 2.5)$ lies above the chord), which both hold for Eq. (10) since $a(x)$ is a continuous function. Hence, this is the unique steady-state solution for the given flux f_{thick} (if any other concentration distribution is used as initial data, for example, obtained by jumping between the flux curves in any other order, then Eq. (4) will be violated and Eq. (10) will produce a non-stationary solution).

In the boundary case $f_{thick} = f(u_M) = f(u_m)$ the steady-state solution is uniquely determined in the interval $(2, 4)$ but the discontinuity is arbitrarily located in $[0, 2]$ (see Figs. 5 and 6). Note that $u_s(2+0) = u_M$ and $u'_s(2+\varepsilon) \to \infty$ as $\varepsilon \to 0+$.

It should now be clear that for $u_s(2) < u_M$ the largest f_{thick} the thickening zone can handle is $f(u_M) = f(u_m) = 6.25$ kg/(m^2 h). A value of f_{thick} above $f(u_M)$ ($u_s(2) < u_M$) is not possible in steady state, because there is no flux curve $f_a(\cdot, x)$ above the minimum point $((u_M, f(u_M))$ for any x. The only possibility to reach the outlet flux $f_u(u) = vu \approx f_a(u, D)$ is to make a jump from a lower concentration to a higher with a chord above the flux curve and this violates the entropy condition (Eq. (4)). *Consequently, in the region* $(0, d]$ *there is no concentration in the interval* (u_m, u_M) *at any steady-state situation.*

If $u_s(d) \in [u_M, u_{max}]$ then, necessarily, the steady-state flux in the thickening zone $f_{thick} \in [f(u_M), f(u_{max})]$. The only possibility for a discontinuity is at the feed level $x = 0$ (see Fig. 7(right)).

3.1.2. When does a discontinuity appear in the compaction zone?

We have seen that for low values of f_{thick} the steady-state solution in (d, D) is continuously increasing, and for larger values there is a discontinuity, which location is higher (lower x values) the larger f_{thick} is. The discontinuity exists when $f_a(\cdot, x)$ has a local minimum point, which is the case as long as the slope of the flux curve is negative at u_{infl}. If $a(x)$ is strictly decreasing and $f'_b(u_{infl}) < 0$ it follows that the slope at the inflection point:

$$\frac{\partial f_a}{\partial u}(u_{infl}, x) = \frac{a(x)}{A_+} f'_b(u_{infl}) + v,$$

as a function of x is (continuously) increasing from negative values to positive (assuming $a(D) \approx 0$), which is clearly seen in the figures. Hence, there is a unique $x = x_0$ for which this slope is zero:

$$\frac{a(x_0)}{A_+} f'_b(u_{infl}) + v = 0.$$

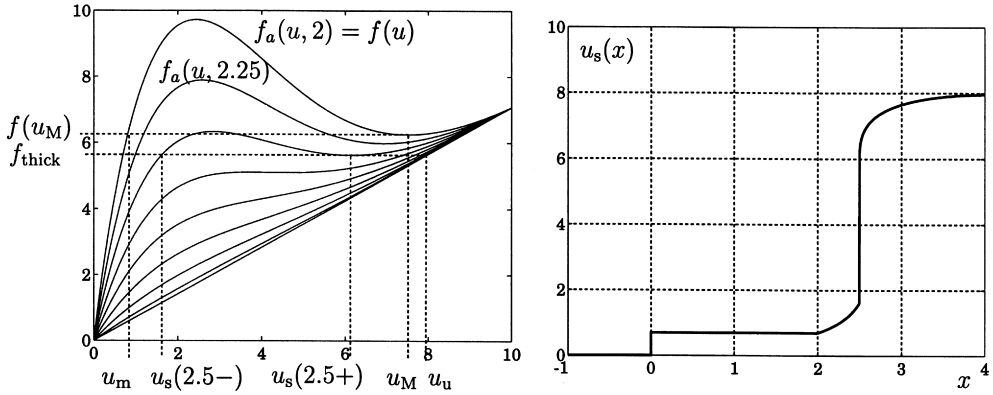

Fig. 4. Left: the third flux function from above is $f_a(u, 2.5$ m); f_{thick}=5.63 kg/(m^2 h). Right: the steady-state solution with a sludge blanket at x=2.5 m (the flux is zero in the clarification zone). The underflow concentration is u_u=f_{thick}/v=7.96 kg/m^3.

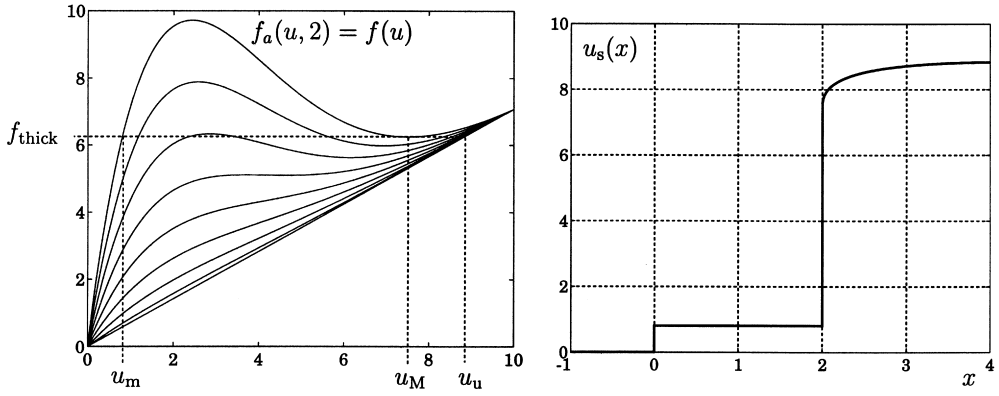

Fig. 5. Left: flux functions and $f_{\text{thick}}=f(u_{\text{M}})=f(u_{\text{m}})=6.25$ kg/(m^2 h). Right: a steady-state solution with a sludge blanket at $x=2$ m (the flux is zero in the clarification zone). Note that $u_{\text{s}}(2-0)=u_{\text{m}}=0.80$ kg/m^3 and $u_{\text{s}}(2+0)=u_{\text{M}}=7.50$ kg/m^3. The underflow concentration is $u_{\text{u}}=f_{\text{thick}}/v=8.83$ kg/m^3.

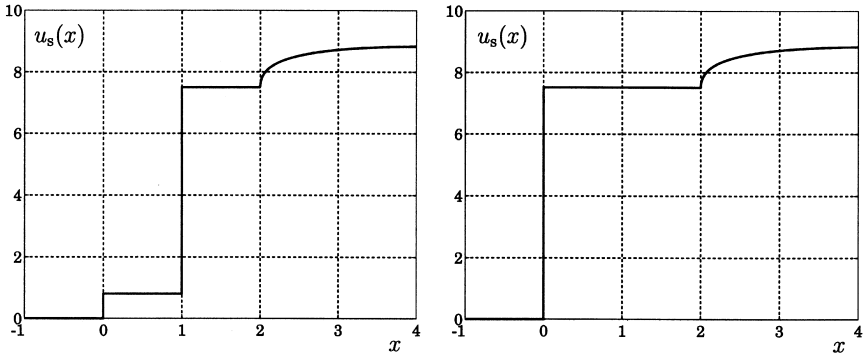

Fig. 6. Two steady-state solutions with $f_{\text{thick}}=f(u_{\text{M}})=\text{f}(u_{\text{m}})=6.25$ kg/(m^2 h).

x_0 is uniquely determined by this equation and it can be used to write the corresponding flux value as:

$$f_{\text{a}}(u_{\text{infl}},\, x_0) = \frac{a(x_0)}{A_+}\, f_{\text{b}}(u_{\text{infl}}) + v u_{\text{infl}} = v\left(u_{\text{infl}} - \frac{f_{\text{b}}(u_{\text{infl}})}{f'_{\text{b}}(u_{\text{infl}})}\right),$$

which is independent of $a(x_0)$. With the numerical data used in the figures, this flux value is 5.05 kg/(m^2 h). Hence, for $0 \le f_{\text{thick}} \le 5.05$ or $f_{\text{thick}} \ge f(u_{\text{M}}) = 6.25$ there is no discontinuity in the compaction zone and for $5.05 < f_{\text{thick}} < f(u_{\text{M}}) = 6.25$ there is one.

3.2. Dynamic boundary concentrations at the bottom

So far we have seen that for the right settler of Fig. 1 the only possibility for the concentration at $x = d$ in a steady-state situation is to lie in $[0,\, u_{\text{m}}]$ or $[u_{\text{M}},\, u_{\max}]$ and

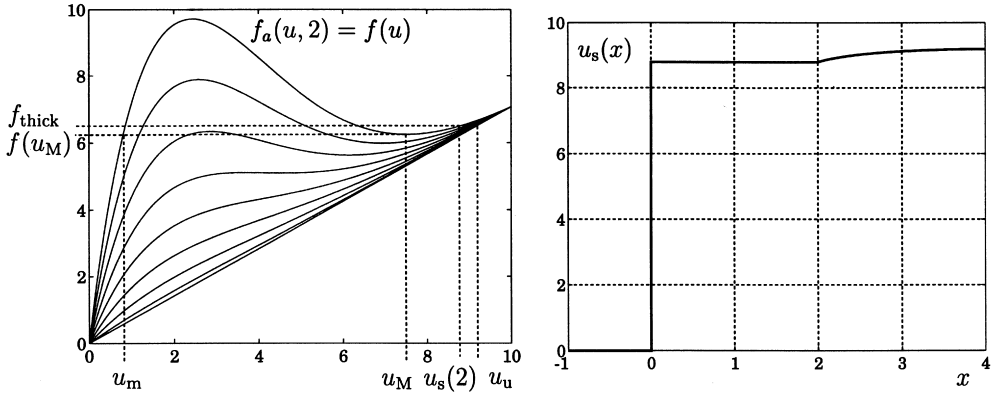

Fig. 7. A steady-state solution with $f_{\text{thick}}=6.50$ kg/(m^2 h) (the flux is zero in the clarification zone). $u_{\text{s}}(x)=8.80$ kg/m^3 for $0<x\le 2$. The underflow concentration is $u_{\text{u}}=f_{\text{thick}}/v=9.19$ kg/m^3.

that the underflow concentration is determined as the intersection of the constant flux f_{thick} within the region $d \le x < D$ and the straight line with slope v.

The reasoning above holds for any $d < D$. In the limit case $d \to D$, corresponding to the left settler model, the only possible boundary concentration at the bottom is still in $[0,\ u_{\text{m}}]$ or $[u_{\text{M}},\ u_{\max}]$. In a dynamic situation this is still true, since the flux is continuous over $x = D$ by the conservation of mass. Hence, we have motivated that the boundary concentration at the bottom satisfies:

$$u^D(t) \in [0,\ u_{\text{m}}] \cup [u_{\text{M}},\ u_{\max}].$$

The conservation law used in a neighbourhood of the bottom $x = D$ (left settler model) can be written:

$$\frac{\partial u}{\partial t} + \frac{\partial f(u)}{\partial x} = 0, \quad x < D \tag{12}$$

$$f(u^D(t)) = f_{\text{u}}(u_{\text{u}}(t)), \quad x = D \tag{13}$$

$$\frac{\partial u}{\partial t} + \frac{\partial f_{\text{u}}(u)}{\partial x} = 0, \quad x > D \tag{14}$$

where $u_{\text{u}}(t)$ is the boundary concentration below $x = D$. The jump condition (Eq. (13)) must be supplemented by an entropy condition, which should be a generalization of Eq. (4) since two different flux functions are involved. Furthermore, the two boundary concentrations $u^D(t)$ and $u_{\text{u}}(t) \equiv \lim_{\varepsilon \to 0+} u(D + 0,\ t + \varepsilon)$ should be determined given initial data only for $x < D$. The generalized entropy condition given in [16] (condition Γ) and its use in the construction of a solution in a neighbourhood of $x = D$ for all possible initial data is described in Section 7.2 of [17]. Here we give the following example.

Assume that the initial datum is the constant $u_0 = 1.5$ (see Fig. 8) above the bottom of the thickening zone, i.e., let $u(x,\ 0) = u_0$ for $x < D$ in the problem (Eqs. (12)–(14)). Note that we do not specify any initial data for $x > D$. As we have motivated above the concentration $u_0 \in (u_{\text{m}},\ u_{\text{M}})$ will not be kept as a boundary concentration any open time interval. The unique solution is constructed in the following way. Given the flux function f above the boundary $x = D$ define the auxiliary function:

$$\breve{f}(u;\ u_0) = \begin{cases} \max_{\alpha \in [u, u_0]} f(\alpha), & 0 \le u \le u_0 \\ \min_{\alpha \in [u_0, u]} f(\alpha), & u_0 < u \le u_{\max}, \end{cases} \tag{15}$$

which is a non-increasing function (see Fig. 8). In a symmetrical way we define an auxiliary non-decreasing function given the flux function below the boundary ($x = D$). Since in the present example f_{u} is already increasing, the auxiliary function $\hat{f}_{\text{u}} = f_{\text{u}}$ independently of any initial data for $x > D$ which, therefore, need not be given. *Condition* Γ*states that the flux at the boundary ($x = D$) is the flux value γ of the intersection of $\breve{f}$ and $\hat{f}_{\text{u}}$, and that the boundary concentrations satisfy*:

$$f(u^D(t)) = \gamma = f_{\text{u}}(u_{\text{u}}(t)).$$

The flux value at the boundary is $\gamma = f(u_{\text{M}}) = 6.2$ (see Fig. 8(left)). The boundary value at the bottom within the settler is $u^D(t) = u_{\text{M}} = 7.5$. The unique solution, which is constructed by the method of characteristics, is shown in Fig. 8(right). From the bottom there is a rising discontinuity, below which the concentration is continuously increasing from $u_0^* = 6.30$ to $u_{\text{M}} = 7.50$. The solution in this region is $u(x,\ t) = (f')^{-1}(\frac{x-D}{t})$ (f' is increasing to the right of the inflection point, hence invertible for these concentrations). u_0^* is defined as the concentration greater than u_0 at which the tangent of the graph of f passes through $(u_0,\ f(u_0))$ (for a strict definition see Ballou [2]). Because of the increasing function f_{u} the characteristics in $x > D$ are always directed downwards (in the positive x-direction). Hence, initial data need not be given for $x > D$. The boundary value $u_{\text{u}}(t)$ is uniquely determined by Eq. (13), which gives:

$$u_{\text{u}}(t) = \frac{f\left(u^D(t)\right)}{v} = u^D(t) + \frac{f_{\text{b}}\left(u^D(t)\right)}{v} = 8.83\,\text{kg/m}^3.$$

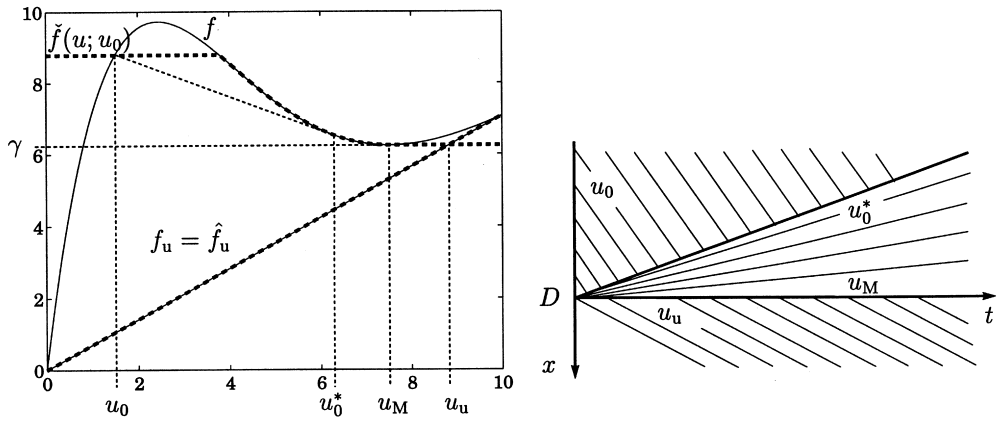

Fig. 8. The use of condition Γ at the bottom of the left settler model. Left: flux functions and auxiliary functions (thick dashed). Right: solution shown by characteristics (thin lines) and discontinuities (thick lines).

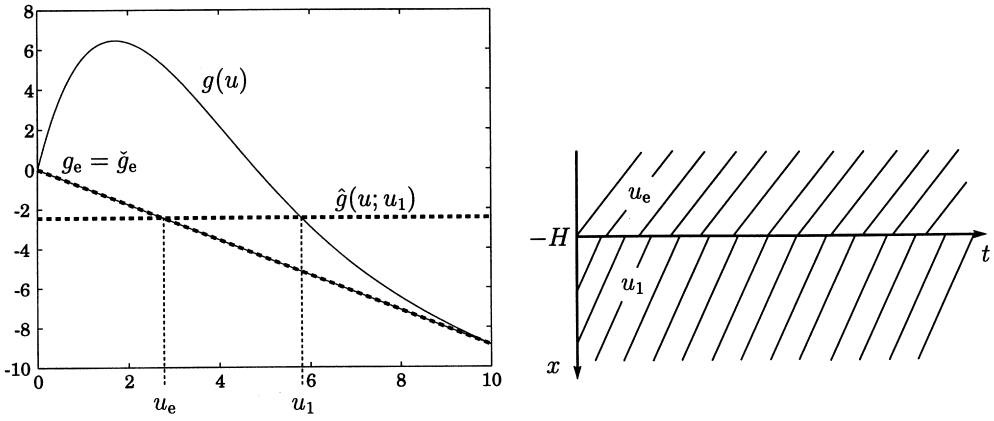

Fig. 9. Left: flux functions, auxiliary functions (thick dashed) and the concentrations u_1=5.73 kg/m^3, u_e=2.56 kg/m^3. Right: the solution satisfying condition Γ. Note that the slopes of the characteristics are $(A_+/A_-)\,g_e'(u_e)=-Q_e/A_-$ (for $x<-H$), which is the bulk velocity, and $(A_+/A_-)\,g_e'(u_1)=-Q_e/A_-$ (for $x>-H$) because of the definition of the flux functions (Eq. (6)).

The example above holds qualitatively for any $u_0 \in (u_m,\ u_M)$ with the addition that if $u_0 \in [u_{infl},\ u_M)$ then u_0^* is replaced by u_0 and the previously rising discontinuity is a line of continuity instead.

If $u_0 \in [0,\ u_m] \cup [u_M,\ u_{max}]$ then the bottom concentration is the constant u_0 and the underflow concentration is $u_u = f(u_0)/v$. We omit the details of this and the cases in which the concentration is not constant above the bottom and refer to [17].

3.3. Boundary concentrations at the top

The handling of the concentrations at the effluent is analogous to the way the boundary concentrations at the underflow were treated above. The conservation law for the region $x < -H$ is:

$$\frac{\partial u}{\partial t} - \frac{Q_e}{A_-}\frac{\partial u}{\partial x} = 0,$$

which is a linear convection equation that carries away the boundary concentrations $u_e(t) \equiv \lim_{\varepsilon\to 0+} u(-H-0,\ t+\varepsilon)$ from the boundary $x = -H$ (to lower x values in the x–t plane) with the bulk speed Q_e/A_-. The construction of a solution involves the auxiliary functions $\check{g}_e = g_e$ and $\hat{g}$, cf. [17]. For example, assume that a discontinuity with the constant concentration $u_1 = 5.72$ below has reached the top of the settler at $t = 0$, that is, the initial concentration is u_1 in the (upper part of the) clarification zone. The unique solution thereafter is shown in Fig. 9. The boundary concentration at the top within the settler is $u^H(t) = u_1$ and the effluent concentration is given by the jump condition (Eq. (8)), which gives:

$$u_e(t) = u^H(t) - \frac{A_- f_b\left(u^H(t)\right)}{Q_e}. \tag{16}$$

Hence, u_e is less than u^H (or equal if $u^H = 0$ or u_{max}). This is due to the fact that the particles within the clarification zone settle. In fact, if the gravity settling force downwards is balanced by the liquid's drag force upwards, then it is possible to have a non-zero concentration of particles at the very top of the clarification zone and still have a zero effluent concentration.

3.4. Boundary concentrations at the feed level

The most complicated situations occur at the feed level. The jump condition (Eq. (7)) is not sufficient to determine the two boundary concentrations u^- above and u^+ below the feed level. Given initial data at $t = 0$ with u_- and u_+ the limit concentration above and below $x = 0$ respectively, form the auxiliary non-increasing function $\check{g}(u;\ u_-)$, cf. (Eq. (15)), and the non-decreasing function:

$$\hat{f}(u;\ u_+) = \begin{cases} \min_{\alpha\in(u,u_+)} f(\alpha), & 0 \le u \le u_+ \\ \max_{\alpha\in(u_+,u)} f(\alpha), & u_+ < u \le u_{max}. \end{cases}$$

Condition Γ *states that, for every fixed* t *the flux at* $x = 0$ *is the flux value* $\gamma(t)$ *of the intersection of* $\check{g}(\cdot;\ u_-(t)) + s(t)$ *and* $\hat{f}(\cdot;\ u_+(t))$ *and that the boundary concentrations satisfy:*

$$f(u^+(t)) = \gamma(t) = g(u^-(t)) + s(t).$$

Note that the latter equation may be satisfied by several candidates of u^+ and u^-, however, only one pair can be used as limit concentrations of a solution. This is described (and proved) generally in [17] and in the next section we show the procedure of construction by examples.

4. Construction of global solutions

In the two following examples we consider the left settler model of Fig. 1 filled with only liquid, that is, with zero concentration as the initial data. The settler is fed with two

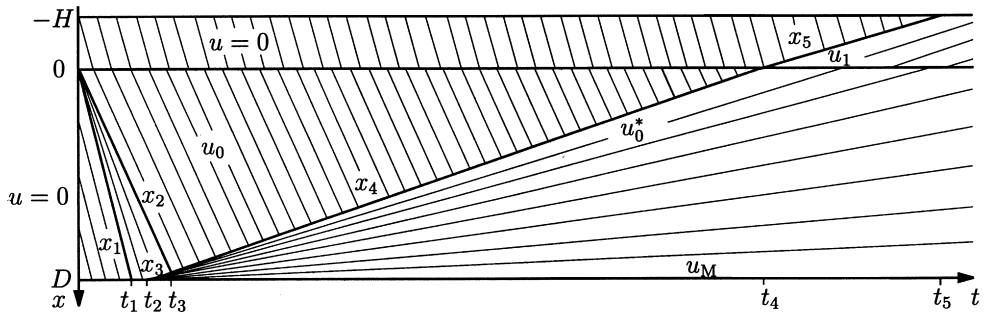

Fig. 10. Example 1. The solution in the case a settler is filled with solids at a constant rate. Thin lines are characteristics and thick lines are discontinuities except for x_1 and x_2, which are lines of continuity.

different constant concentrations, which both result in overflow situations. To construct solutions in a neighbourhood of the feed inlet we conclude from the jump condition (Eq. (7)) (and condition Γ) that it is convenient to draw the graphs of $f(u)$and $g(u)+s$ (and their auxiliary functions) in the same figure. We also remark that in the case of a continuous $A(x)$ at $x = 0$ the feed concentration is the intersection of these graphs. In the present case $A_+ \approx A_-$ and u_f is approximately the intersection. This is because the concentration value $u^i$of an intersection satisfies $f(u^i) = g(u^i) + s$ and:

$$u_\mathrm{f} = \frac{A_+ s}{Q_\mathrm{f}} = \frac{A_+}{Q_\mathrm{f}}\left(f(u^i) - g(u^i)\right)$$
$$= \frac{A_+}{Q_\mathrm{f}}\left(f_\mathrm{b}(u^i) + \frac{Q_\mathrm{u}}{A_+}u^i - \frac{A_-}{A_+}f_\mathrm{b}(u^i) + \frac{Q_\mathrm{e}}{A_+}u^i\right)$$
$$= u^i + \frac{A^+ - A_-}{Q_\mathrm{f}}f_\mathrm{b}(u^i),$$

where we have used that $Q_\mathrm{u} + Q_\mathrm{e} = Q_\mathrm{f}$. The highest value of the last term for the simulations in this paper is $\frac{A_+ - A_-}{Q_\mathrm{f}} \max_{0\le u\le u_\mathrm{max}} f_\mathrm{b}(u) = 0.02$ kg/m^3, hence $u_\mathrm{f} \approx u^i$.

Example 1. A settler with the initial concentration zero is fed with a constant concentration. The numerical values are:

$u_\mathrm{f} = 5.52$ kg/m^3
$s = 8.79$ kg/(m^2 h)
$u_0 = 1.50$ kg/m^3
$u_0^* = 6.30$ kg/m^3
$u_1 = 5.73$ kg/m^3
$u_\mathrm{u} = 8.83$kg/m^3
$u_\mathrm{e}(\infty) = 2.87$ kg/m^3

and the solution is shown in Fig. 10 in terms of characteristics and discontinuities.

The graphs of $f(u)$ and $g(u) + s$ are shown in Fig. 11 together with those of $\hat{f}(u;\ 0)$ and $\check{g}(u;\ 0)+s$. The intersection of the graphs of these two auxiliary functions occurs at the concentration u_0 and the flux value $\gamma = s$. The (unique) boundary concentrations are $u^+(t) = u_0$ and $u^-(t) = 0$ for $t > 0$ until any wave of another concentration reaches $x = 0$, which occurs at $t = t_4$. The reason for this is that $\hat{f}(\cdot;\ u_0) \equiv \hat{f}(\cdot;\ 0)$ holds, which implies that the graphs and implications of Fig. 11 hold for every $t \in (0,\ t_4)$. The solution is therefore zero in the clarification zone for $0 \le t < t_4$.

Between the straight lines $x_1 = f'(0)t$ and $x_2 = f'(u_0)t$ there is an expansion wave consisting of all concentrations between zero (along x_1 and u_0 (along x_2). The expansion wave can be expressed as $u(x,\ t) = (f')^{-1}\,(x/t)$ (since f' is decreasing to the left of the inflection point, it is invertible for these concentrations).

At the bottom the concentration increases continuously from zero after the time point t_1 see Fig. 12(left), and so does $u_\mathrm{u}(t)$. Let t_2 denote the time point for which $u_D(t_2) = u_\mathrm{m}$ and $u^D(t_2) = u_\mathrm{M}$. For $t > t_2$ the boundary concentration is $u_D(t) = u^D(t) = u_\mathrm{M}$. At $t = t_2$, a discontinuity x_3 emanates from the bottom with the initial velocity zero (there is a jump between u_m and u_M and the final velocity:

$$x_3'(t_3) = \frac{f(u_0^*) - f(u_0)}{u_0^* - u_0}$$

which is also the slope of the discontinuity x_4. During $t_2 < t < t_3$ the concentration above x_3 increases from u_m to u_0 and the concentration below decreases from u_M (at the bottom) to u_0^*, cf. Fig. 12(right). The solution in the thickening zone to the right of x_3 and x_4 is defined by the character-

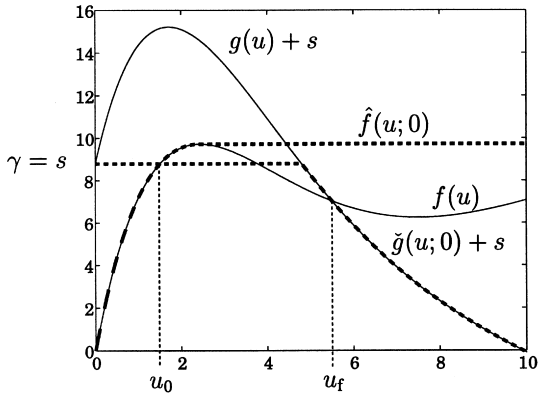

Fig. 11. Example 1. The situation at the feed level at t=0. The initial boundary values are $u_-(0)$=$u_+(0)$=0. Note that u_f is (approximately) the intersection of the two graphs.

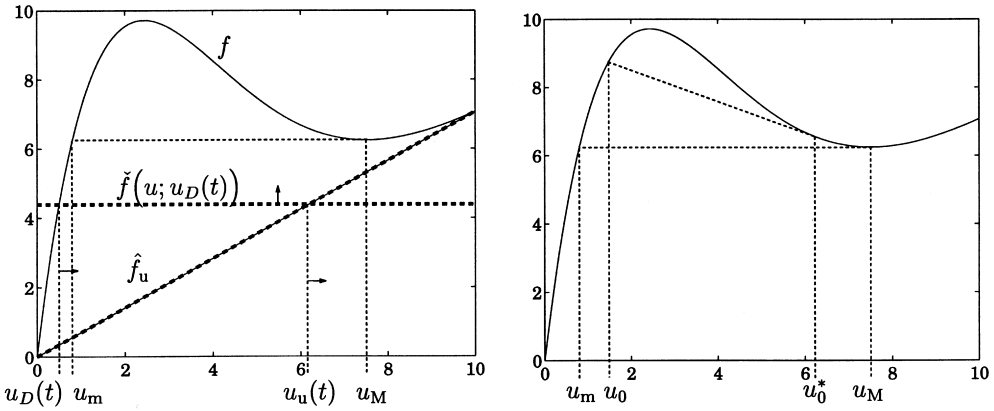

Fig. 12. Example 1. Left: the situation at the bottom at a time point $t \in (t_1, t_2)$. The small arrows show the directions of movement with increasing time. Right: the concentrations appearing above x_3 are $[u_m, u_0]$ and below are $[u_0{}^*, u_M]$.

istics that emanate tangentially from x_3 (which is called a contact discontinuity).

At $t = t_4$ the discontinuity x_4 reaches the feed level and the situation there changes. The graphs of $\hat{f}(u; u_0^*)$ and $\check{g}(u; 0) + s$ are shown in Fig. 13. The intersection of these two graphs occurs at the flux value $\gamma(t_4) = f(u_0^*)$ and the concentration u_1 which is the solution of:

$$g(u_1) + s = f(u_0^*).$$

The new boundary concentration in the clarification zone is $u^-(t_4) = u_1$ yielding characteristics emanating from the feed level upwards. The boundary concentration below the feed level is continuous at t_4: $u^+(t_4) = u_+(t_4) = u_0^*$. After this time point $u_+(t)$ increases asymptotically up to $u_M$at $t = \infty$ which implies that the concentration $u_-(t)$ is slightly increasing up to its limit value $u_2 > u_1$ determined by the intersection of $f(u_M)$ (the flux value of the plateau of $\hat{f}(u; u_M)$ and $g(u) + s$. We leave the details of forming $\hat{f}(\cdot; u_+(t))$ and $\check{g}(\cdot; u_-(t)) + s$ etc. to the reader.

At $t = t_5$ the discontinuity x_5 reaches the top of the settler resulting in an overflow and the situation shown in Fig. 9 holds, except for the fact that the boundary concentration at the top is now increasing slightly above u_1 as $t \to \infty$.

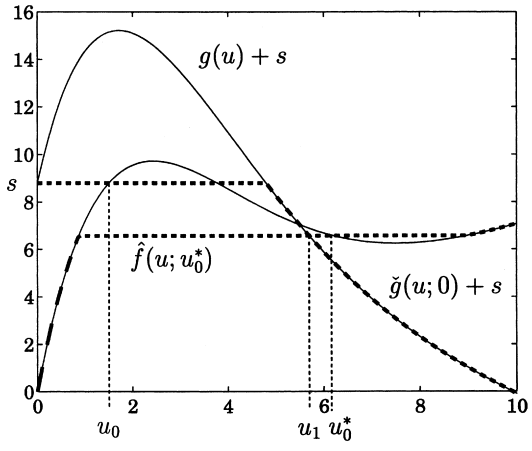

Fig. 13. Example 1. The situation at the feed level at $t = t_4$.

Example 2. In this example the initial data and values of the volume flows are the same as in Example 1 except for a higher feed concentration. The numerical values are:

$u_f = 6.91$ kg/m^3
$s = 11$ kg/(m^2 h)
$u_0 = 2.44$ kg/m^3
$u_0^* = 5.27$ kg/m^3
$u_1 = 5.31$ kg/m^3
$u_2 = 6.43$kg/m^3
$u_e(t_3) = 1.45$ kg/m^3
$u_e(\infty) = 5.38$ kg/m^3
$u_u = 8.83$ kg/m^3

and the solution is shown in Fig. 14. The initial situation at the feed level is shown in Fig. 15. The intersection between the two dashed graphs occurs at the flux value $\gamma = f(u_0)$ where u_0 is the concentration of the local maximum point of f. Note that in this example $s > f(u_0)$ which implies that solids will be transported into the clarification zone immediately. The (unique) boundary concentrations at the feed level are $u^+(t) = u_0$ and $u^-(t) = u_1$ for $0 \le t < t_4$.

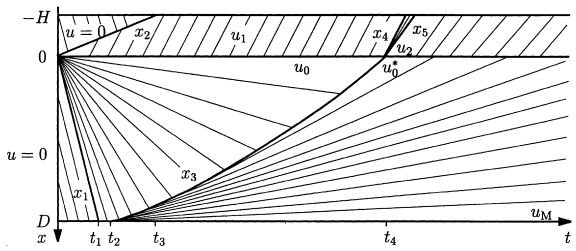

Fig. 14. Example 2. The solution in the case of a higher feed concentration than in Example 1. Thin lines are characteristics and thick lines are discontinuities except for x_1, x_4 and x_5, which are lines of continuity.

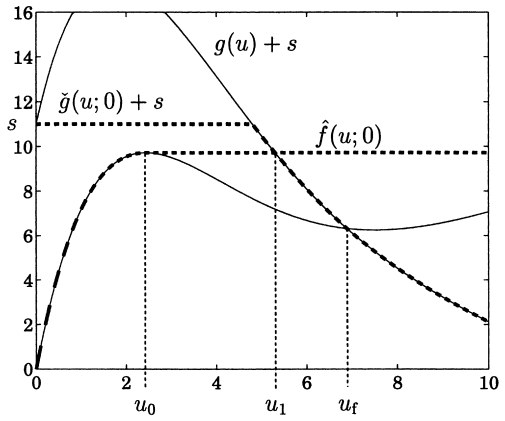

Fig. 15. Example 2. The situation at the feed level at t=0.

In the clarification zone a shock wave x_2 is immediately formed having the velocity:

$$x_2'(t) = \frac{g(u_1) - g(0)}{u_1 - 0} = \frac{g(u_1)}{u_1} < 0$$

according to the jump condition. Hence, it reaches the effluent level at the time point:

$$t_3 = \frac{Hu_1}{-g(u_1)}.$$

In the thickening zone there is an expansion wave similar to the one in Example 1, but this one is spread up to the feed level since the characteristic with concentration u_0 has zero slope. The solution in the thickening zone on the right of x_3 is defined by the characteristics that emanate tangentially from x_3. The concentration on the right of x_3 decreases with height from u_M (at the bottom) to u_0^* at $(x, t) = (0, t_4)$.

The discontinuity x_3 reaches the feed level at t_4. The new boundary concentration in the clarification zone $u^-(t_4) = u_2$ is defined by the intersection of the graphs shown in Fig. 16, hence it can be obtained as the solution of:

$$f(u_0^*) = g(u_2) + s.$$

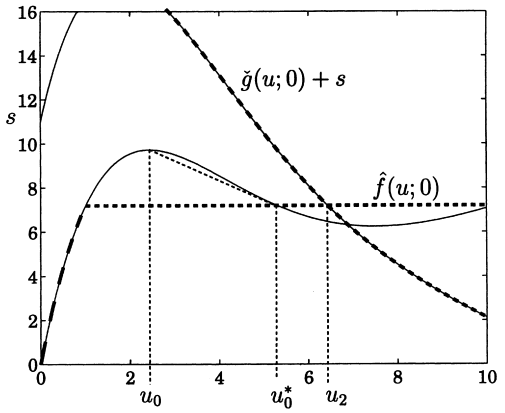

Fig. 16. Example 2. The situation at the feed level at t=t_4.

The situation at the feed level after $t = t_4$ is qualitatively the same as in Example 1. In the clarification zone there is a small expansion wave between x_4 and x_5 separating the concentrations $u_1$and u_2. Since, in this example, $u_1 > u_{infl}$, x_4 is a line of continuity. If $u_1 < u_{infl}$, then x_4 would be a discontinuity instead with the concentration u_1^* (defined by drawing a tangent as shown previously) on the right.

The situation at the bottom is the same as in Example 1, and the effluent concentration is calculated from Eq. (16); cf. the numerical solution in Fig. 20.

5. Numerical solutions

The numerical method described in [19,20] is used. It is based on Godunov's [24] method, in which the concentration related to each grid point along the x-axis at a certain time

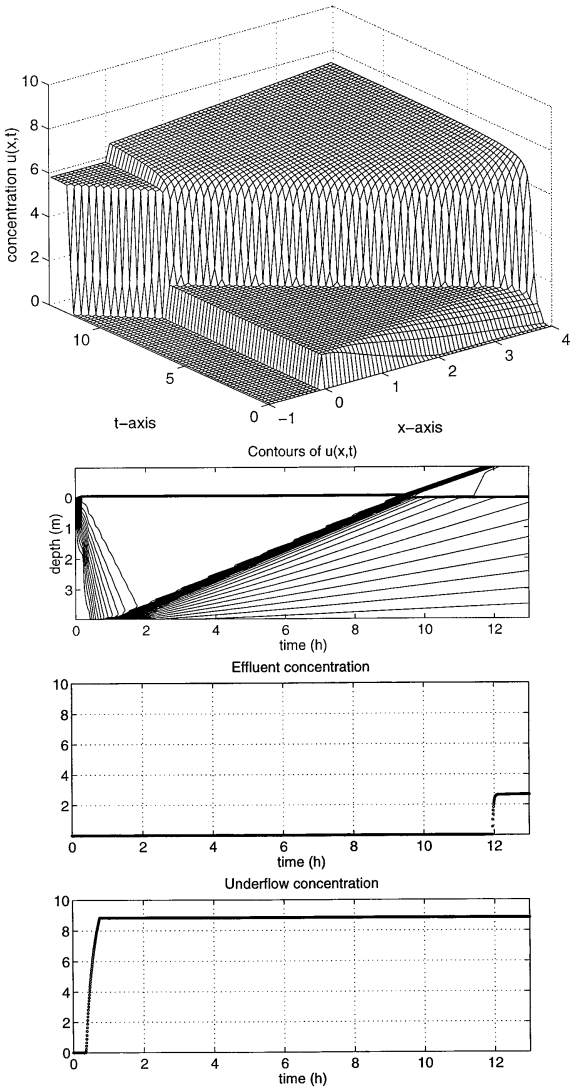

Fig. 17. Example 1. Numerical solution corresponding to the analytical one of Fig. 10.

point is the average of an analytical solution originating from piecewise constant initial data at the preceding time point. It is a conservative method, which means that although discontinuities are smoothed (by numerical diffusion), they are located correctly, that is, they move with the correct speed.

Example 1, continued. Fig. 17 shows the numerical solution when the left settler model is filled with solids. With the same initial data and feed concentration Fig. 18 shows the numerical solution for the right settler model. Since the volume of this settler is less than the other one, it cannot keep as much mass and is thus filled up faster. In order to investigate the limit case $d \to D$ numerically we present in Fig. 19 the numerical solutions for different values of d. We should mention that although numerical simulations are possible for the right settler model, a drawback is that the upper bound on the time step length tends to zero as the cross-sectional area $a(D)$ tends to zero; cf. [17]. This is because of the bulk velocity $Q_u/a(D)$ at the bottom, which carry information very fast as $a(D)$ is small.

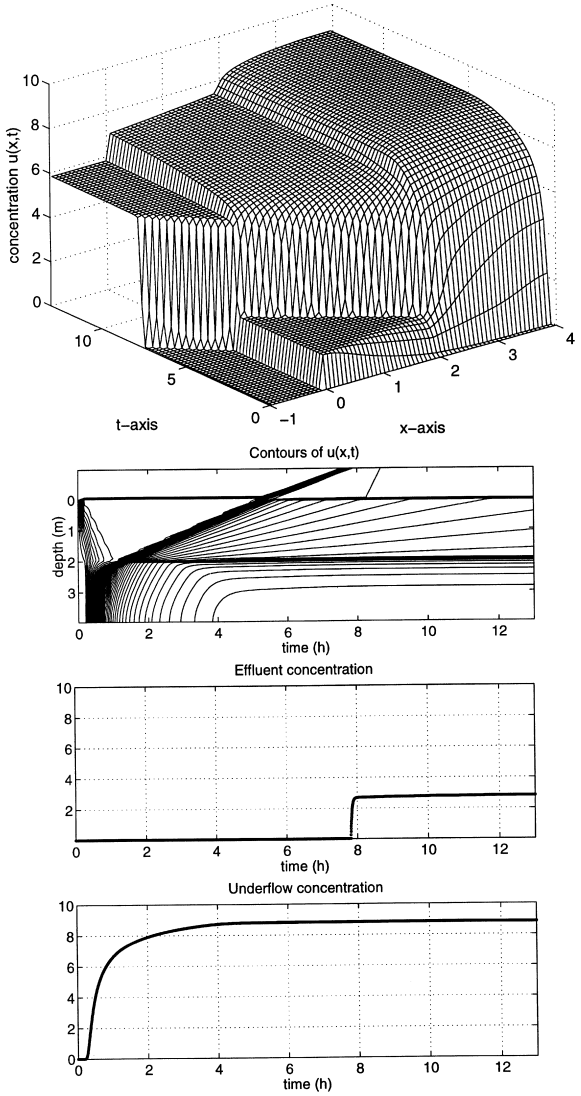

Fig. 18. Numerical solution of Example 1 in the case of a compaction zone between x=d=2 and 4 m.

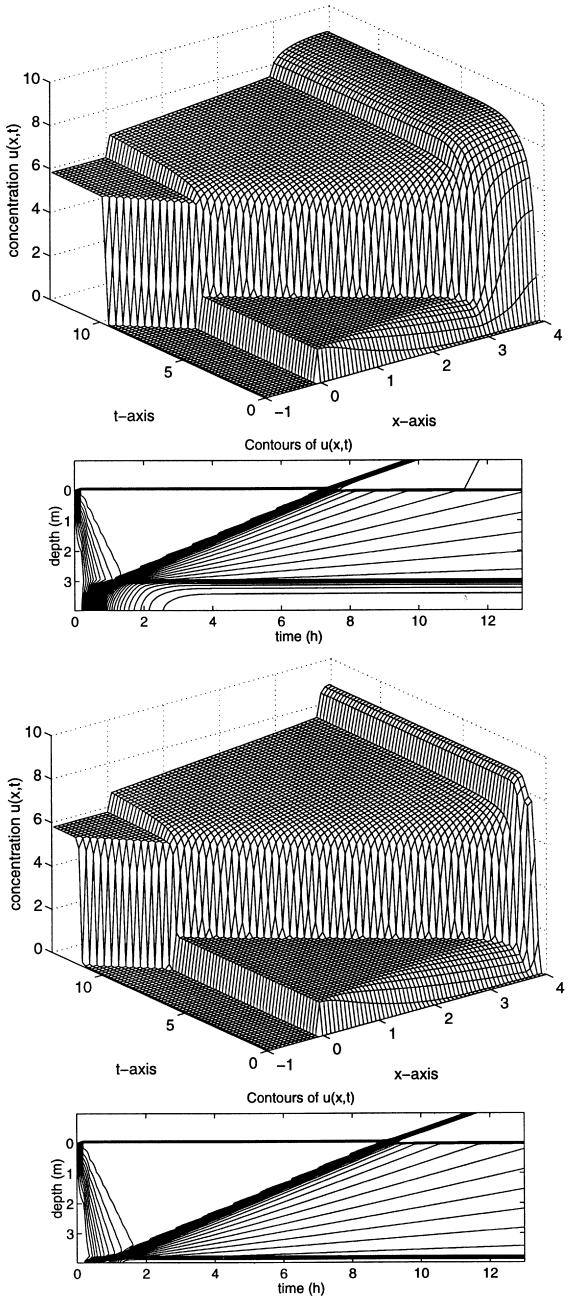

Fig. 19. Numerical solutions in the case of a compaction zone with d=3 m (upper) and 3.8 m (lower).

Example 2, continued. The numerical solution is shown in Fig. 20 for the left settler model. Note that the high feed concentration implies in this case that solids are building up immediately in the clarification zone. This is an example showing non-monotone concentration distributions during a

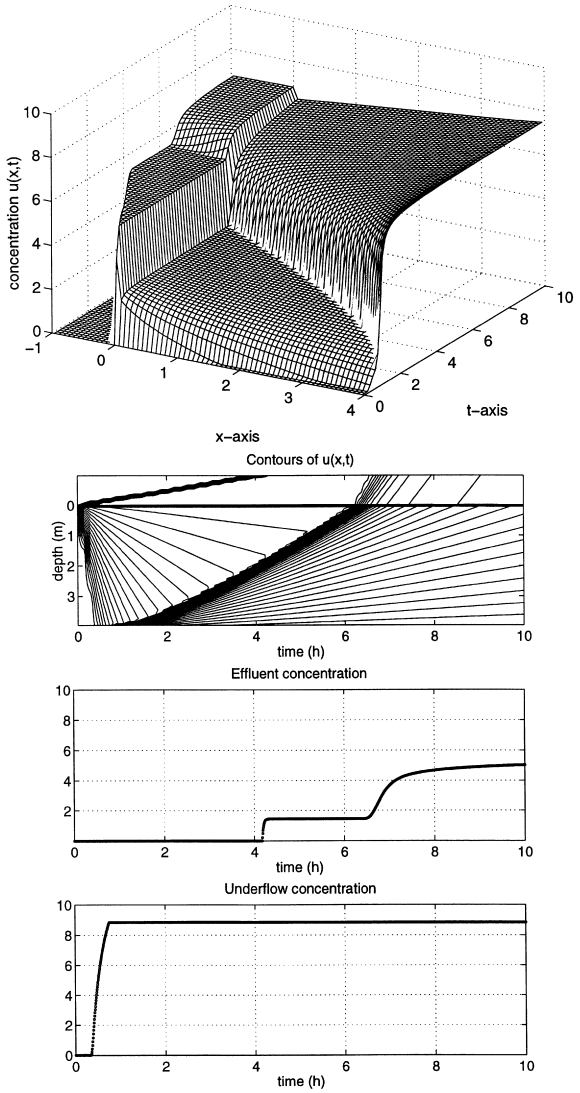

Fig. 20. Example 2. Numerical solution corresponding to the analytical one of Fig. 14. Note the different direction from which the three-dimensional graph is shown.

long part of the transient. However, the final steady-state solution is non-decreasing with depth, which is generally true for a settler with non-increasing cross-sectional area.

6. Conclusions

The restriction to one dimension in the modelling of continuous sedimentation means that several idealized assumptions are made. Usually the cross-sectional area is assumed to be constant all the way down to the bottom. This is advantageous when constructing solutions analytically as well as numerically (assuming the Kynch constitutive assumption holds). However, the situations at the inlet and outlets are complex even for such an ideal model. For example, the discontinuity between the bottom concentration and the underflow concentration under normal operating conditions has been discussed in the literature and different conditions have been suggested to hold in dynamical situations. In this paper it has been shown that this discontinuity is a natural consequence of the ideal model by considering a model with a converging cross-sectional area at the bottom (compaction zone). Concurrently, the increase of concentration in the compaction zone only due to the gravity settling (no compression) has been demonstrated, which is in agreement with the earlier results by Shannon and Tory [31]. In reality an increase in concentration at the bottom is observed. However, there are additional phenomena that affect the concentration distribution, e.g. rake action and flows in two or three dimensions.

The generalized entropy condition introduced in [16] resolves the problems of determining the concentrations at the inlet and the outlets (of an ideal model) at any loading condition. The generalized entropy condition is in this paper illustrated by considering a settler model with constant cross-sectional area below the feed level as a limit model of another one with a converging cross-sectional area at the bottom. Mathematically, this means that a discontinuity in flux functions (between f and f_u) has been studied by considering a continuous transition between them. This type of smoothing procedure has been performed in a more general and rigorous way for general flux functions in [18,22], where the addition of a small amount of diffusion is treated simultaneously. The use of this condition in the construction of solution for the entire settler has been demonstrated in two examples accompanied by numerical solutions.

Acknowledgements

I am grateful to Prof. Elmer M. Tory for reviewing the manuscript carefully and giving valuable corrections and additions. I also acknowledge Dr Ulf Jeppsson and Prof. Gunnar Sparr for reading and commenting on the manuscript. This work has been supported by the Swedish Research Council for Engineering Sciences (TFR), project 96-715.

References

[1] F.M. Auzerais, R. Jackson, W.B. Russel, The resolution of shocks and the effects of compressible sediments in transient settling, J. Fluid Mech. 195 (1988) 437–462.
[2] D.P. Ballou, Solutions to nonlinear hyperbolic Cauchy problems without convexity conditions, Trans. Am. Math. Soc. 152 (1970) 441–460.
[3] R. Bürger, F. Concha, Mathematical model and numerical simulation of the settling of flucculated suspensions, Int. J. Multiphase Flow 24 (1998) 1005–1023.
[4] R. Bürger, W.L. Wendland, F. Concha, Modelling equations for gravitational sedimentation-consolidation process, Z. Angew. Math. Mech. 80 (2000) 79–92.
[5] M.C. Bustos, F. Concha, On the construction of global weak solutions in the Kynch theory of sedimentation, Math. Methods Appl. Sci. 10 (1988) 245–264.

[6] M.C. Bustos, F. Concha, W. Wendland, Global weak solutions to the problem of continuous sedimentation of an ideal suspension, Math. Methods Appl. Sci. 13 (1990) 1–22.
[7] M.C. Bustos, F. Paiva, W. Wendland, Control of continuous sedimentation as an initial and boundary value problem, Math. Methods Appl. Sci. 12 (1990) 533–548.
[8] J.-Ph. Chancelier, M. Cohen de Lara, C. Joannis, F. Pacard, New insight in dynamic modelling of a secondary settler — I. Flux theory and steady-states analysis, Wat. Res. 31 (8) (1997) 1847–1856.
[9] J.-Ph. Chancelier, M. Cohen de Lara, C. Joannis, F. Pacard, New insight in dynamic modelling of a secondary settler — II. Dynamical analysis, Wat. Res. 31 (8) (1997) 1857–1866.
[10] J.-Ph. Chancelier, M. Cohen de Lara, F. Pacard, Analysis of a conservation pde with discontinuous flux: A model of settler, SIAM J. Appl. Math. 54 (4) (1994) 954–995.
[11] D. Chang, T. Lee, Y. Jang, M. Kim, S. Lee, Non-colloidal sedimentation compared with Kynch theory, Powder Technol. 92 (1997) 81–87.
[12] E.W. Comings, Thickening calcium carbonate slurries, Ind. Eng. Chem. 32 (5) (1940) 663–668.
[13] E.W. Comings, C.E. Pruiss, C. De Bord, Continuous settling and thickening, Ind. Eng. Chem. Des. Process. Dev. 46 (1954) 1164–1172.
[14] F. Concha, M.C. Bustos, A. Barrentios, Phenomenological theory of sedimentation, E. Tory (Ed.), Sedimentation of Small Particles in a Viscous Fluid, Computational Mechanics Publications, Southampton, 1956, pp. 51–96.
[15] K.E. Davis, W.B. Russel, W.J. Glantschnig, Settling suspensions of colloidal silica: Observations and X-ray measurements, J. Chem. Soc. Faraday Trans. 87 (3) (1991) 411–424.
[16] S. Diehl, On scalar conservation laws with point source and discontinuous flux function, SIAM J. Math. Anal. 26 (6) (1995) 1425–1451.
[17] S. Diehl, A conservation law with point source and discontinuous flux function modelling continuous sedimentation, SIAM J. Appl. Math. 56 (2) (1996) 388–419.
[18] S. Diehl, Scalar conservation laws with discontinuous flux function: I. The viscous profile condition, Comm. Math. Phys. 176 (1996) 23–44.
[19] S. Diehl, Dynamic and steady-state behaviour of continuous sedimentation, SIAM J. Appl. Math. 57 (4) (1997) 991–1018.
[20] S. Diehl, U. Jeppsson, A model of the settler coupled to the biological reactor, Wat. Res. 32 (2) (1998) 331–342.
[21] S. Diehl, G. Sparr, G. Olsson. Analytical and numerical description of the settling process in the activated sludge operation. In: R. Briggs (Eds.), Instrumentation, Control and Automation of Water and Wastewater Treatment and Transport Systems, IAWPRC, Pergamon Press, 1990.
[22] S. Diehl, N.-O. Wallin, Scalar conservation laws with discontinuous flux function: II. On the stability of the viscous profiles, Comm. Math. Phys. 176 (1996) 45–71.
[23] J.B. Farrow, R.R.M. Johnston, K. Simic, J.D. Swift, Consolidation and aggregate densification during gravity thickening, Chem. Eng. J. 80 (2000) 141–148.
[24] S.K. Godunov, A finite difference method for the numerical computations of discontinuous solutions of the equations of fluid dynamics, Mat. Sb. 47 (1959) 271–306 (in Russian).
[25] G.J. Kynch, A theory of sedimentation, Trans. Faraday Soc. 48 (1952) 166–176.
[26] P.D. Lax, Hyperbolic systems of conservation laws and the mathematical theory of shock waves, SIAM Regional Conference Series Lectures in Appl. Math., No. 11, SIAM, Philadelphia, 1973.
[27] O.A. Oleinik, Uniqueness and stability of the generalized solution of the Cauchy problem for a quasi-linear equation, Uspekhi Mat. Nauk. 14 (1959) 165–170.
[28] O.A. Oleinik, Uniqueness and stability of the generalized solution of the Cauchy problem for a quasi-linear equation, Am. Math. Soc. Trans. Ser. 2 (33) (1964) 285–290.
[29] C.A. Petty, Continuous sedimentation of a suspension with a nonconvex flux law, Chem. Eng. Sci. 30 (1975) 1451.
[30] H.K. Rhee, R. Aris, N. Amundson, First-Order Partial Differential Equations, vol. 1, Prentice-Hall, Englewood Cliffs, NJ, 1986.
[31] P.T. Shannon, E.M. Tory, The analysis of continuous thickening, SME Trans. 235 (1966) 375–382.
[32] J. Smoller, Shock Waves and Reaction–Diffusion Equations, Springer-Verlag, 1983.